 OpenAccess

Preclinical efficacy spectrum and pharmacokinetics of ixabepilone

**Francis Y. F. Lee · Richard Smykla · Kathy Johnston · Krista Menard ·
Kelly McGlinchey · Russell W. Peterson · Amy Wiebesiek · Gregory Vite ·
Craig R. Fairchild · Robert Kramer**

Abstract

Purpose Ixabepilone, a semisynthetic analog of natural epothilone B, was developed for use in cancer treatment. This study extends previous findings regarding the efficacy of ixabepilone and its low susceptibility to tumor resistance mechanisms and describes the pharmacokinetics of this new antineoplastic agent.

Methods The cytotoxicity of ixabepilone was assessed in vitro in breast, lung, and colon tumor cell lines and in vivo in human xenografts in mice. Antitumor activities of ixabepilone and taxanes were compared in multidrug-resistant models in vivo. Differential drug uptake of ixabepilone and paclitaxel was assessed in a P-glycoprotein (P-gp)-resistant colon cancer model in vitro. The pharmacokinetic profile of ixabepilone was established in mice and humans.

Results Ixabepilone demonstrated potent cytotoxicity in a broad range of human cancer cell lines in vitro and in a wide range of xenografts in vivo. Ixabepilone was $\sim$3-fold more potent than docetaxel in the paclitaxel-resistant Pat-21 xenograft model (resistant due to overexpression of βIII-tubulin and a lack of βII-tubulin). Ixabepilone activity against P-gp-overexpressing breast and colon cancer was confirmed in in vivo models. Cellular uptake of ixabepilone, but not paclitaxel, was established in a P-gp-overexpressing model. The pharmacokinetics of ixabepilone was characterized by rapid tissue distribution and extensive tissue binding.

Conclusions Cytotoxicity studies against a range of tumor types in vitro and in vivo demonstrate that ixabepilone has potent and broad-spectrum antineoplastic activity. This is accompanied by favorable pharmacokinetics. Ixabepilone has reduced susceptibility to resistance due to P-gp overexpression, tubulin mutations, and alterations in β-tubulin isotype expression.

Introduction

Since chemotherapy was first developed for the treatment of cancer over four decades ago, a wide range of effective agents have been identified. Despite these advances, the therapeutic benefits of chemotherapy have been limited by the ability of tumors to develop drug resistance [1]. If tumor cells are repeatedly exposed to an antineoplastic agent, cross-resistance to related agents of the same drug class generally is seen. However, the tumor is likely to remain sensitive to drugs from different classes due to their different mechanisms of action [2]. Even so, in many cases, tumors display multidrug resistance (MDR), where cross-resistance occurs to multiple drugs that are neither structurally nor functionally related, and to which the tumor has never been exposed.

Several different mechanisms exist whereby tumors become drug-resistant. One key mechanism is overexpression of the P-glycoprotein (P-gp) efflux pump (encoded by *MDR1*), which can result in subtherapeutic concentrations of cytotoxic agents such as anthracyclines and taxanes being retained in tumor cells [3, 4]. For drugs that

F. Y. F. Lee (✉) · R. Smykla · K. Johnston · K. Menard ·
K. McGlinchey · R. W. Peterson · A. Wiebesiek · G. Vite ·
C. R. Fairchild · R. Kramer
Oncology Drug Discovery, Bristol–Myers Squibb
Pharmaceutical Research Institute, P.O. Box 4000, K22-03,
Princeton, NJ 08540, USA
e-mail: francis.lee@bms.com

 Springer

target microtubules, such as taxanes, other key mechanisms of resistance include overexpression of the βIII-tubulin isotype and tubulin mutations [5, 6]. Multidrug resistance poses a significant challenge to the treatment of cancer and drives the continued search for new compounds without such limitations.

The epothilones are a novel class of microtubule-stabilizing agents produced by the myxobacterium *Sorangium cellulosum*. Four main natural epothilones are produced by *S. cellulosum*: A and B and, to a lesser extent, C and D [7]. These 16-membered macrolide antibiotics are highly effective at inducing cell arrest at the G_2/M phase, resulting in apoptosis [8, 9]. However, although the naturally occurring epothilones demonstrate impressive activity in vitro, it has been difficult to demonstrate antitumor activity in vivo [10]. This is, at least in part, due to the unfavorable pharmacokinetic characteristics and relatively narrow therapeutic window of the naturally occurring epothilones.

Ixabepilone is a semisynthetic analog of epothilone B, chemically modified to retain the highly favorable in vitro characteristics of natural epothilone B while improving the pharmacokinetic profile [11]. Specifically, the lactone oxygen is replaced with a lactam. In previous studies, ixabepilone has demonstrated the ability to overcome tumor resistance due to a range of mechanisms in vivo, showing antitumor activity in the following established models: Pat-7 ovarian carcinoma, HCT116/VM46 human colon carcinoma (both resistant due to P-gp overexpression), A2780Tax ovarian carcinoma (resistant due to a tubulin mutation), clinically derived, paclitaxel-resistant Pat-21 breast carcinoma (resistant due to overexpression of βIII-tubulin), and the inherently paclitaxel-refractory murine fibrosarcoma M5076 (unknown mechanism of resistance, non-MDR) [5].

These promising preclinical findings have since translated to the clinic. Single-agent ixabepilone has shown encouraging antitumor activity in a broad range of tumor types during phase I [12–15] and phase II [16–28] clinical trials.

The results reported herein extend these previous reports regarding the preclinical efficacy of ixabepilone, explore the susceptibility of ixabepilone to tumor resistance mechanisms, and describe the pharmacokinetics of this new antineoplastic agent.

Materials and methods

Materials

Chemicals

Ixabepilone and paclitaxel were synthesized in the Oncology Chemistry Department at Bristol–Myers Squibb

Pharmaceutical Research Institute. Unless specified, chemicals and solutions used for the maintenance of cell culture were obtained from GIBCO-BRL (Grand Island, NY). Sterile tissue culture ware was obtained from Corning (New York, NY). All other reagents were obtained from Sigma Chemical Company (St Louis, MO) at the highest grade available.

Drug administration

For administration of ixabepilone to rodents, two different excipients were used: ethanol/water (1:9, v/v) and Cremophor®/ethanol/water (1:1:8, v/v). Ixabepilone was first dissolved in ethanol or a mixture of Cremophor®/ethanol (50:50). Final dilution to the required dosage strength was made less than 1 h before drug administration. For parenteral administration, dilution was made with water so that the dosing solutions contained the specified excipient composition described above. Docetaxel was administered IV Q43d in ethanol/Tween-80/normal saline (1:1:8, v/v) and paclitaxel at Q2D ×5 in Cremophor®/ethanol/normal saline (1:1:8, v/v).

Tumor cell lines and xenografts

All in vitro cell lines were maintained in RPMI 1640 culture medium and 10% fetal bovine serum (FBS), apart from HCT116 human carcinoma and HCT116/VM46 (an MDR variant) [29], which were maintained in McCoy's 5A medium (Gibco BRL) and 10% FBS. The majority of cell lines used in tissue culture studies were obtained from American Type Culture Collection (Manassas, VA).

Subcutaneous (SC) tumors used in nude mice were obtained from the American Type Culture Collection (Manassas, VA), with the exception of the following tumor lines: Pat-7 is derived from an ovarian tumor biopsy from a patient who developed resistance to paclitaxel (Fox Chase Cancer Center, Philadelphia, PA); Pat-14 was provided by the Cancer Institute of New Jersey (New Brunswick, NJ); Pat-21 is derived from a breast biopsy from a patient who failed paclitaxel and was provided by the Cancer Institute of New Jersey (New Brunswick, NJ); and Pat-24, Pat-25, and Pat-26 were derived from pancreatic carcinomas and were provided by the Fox Chase Cancer Center (Philadelphia, PA). Pat-27 is derived from a patient biopsy from a taxane-resistant tumor and provided by Drs. Hait, Hamilton, and Hoffman (Fox Chase Cancer Center, Philadelphia, PA); KPL-4 was provided by Dr. Kurebayashi (Kowasaki Medical School, Japan); L2987 (lung carcinoma) and CD228 (ovarian carcinoma) were derived by Bristol–Myers Squibb/Oncogene Company (Princeton, NJ); GEO (colon carcinoma) was provided by Dr. M. Brattain (Baylor College of Medicine, Houston, TX);

A2780Tax (ovarian carcinoma) was provided by Dr. T. Fojo (National Cancer Institute, Bethesda, MD); MW387 (ovarian carcinoma) was provided by The James P. Wilmot Cancer Center (University of Rochester Medical Center, Rochester, NY); PA354 (ovarian carcinoma) was provided by University of Rochester (Rochester, NY); CWR-22 and LuCap35 (prostate carcinomas) were provided by Dr. R. Vessella (University of Washington, Seattle, WA); and MDA-PCa-2b (prostate carcinoma generated in vitro from bone metastasis-derived, androgen-dependent MDA-PCa-2b human PC cells) was provided by the University of Texas MD Anderson Cancer Center (Houston, TX).

Animals

Rodents were obtained from Harlan Sprague Dawley Company (Indianapolis, IN), and maintained in an ammonia-free environment in a defined and pathogen-free colony. The animal care program of Bristol–Myers Squibb Pharmaceutical Research Institute is fully accredited by the American Association for Accreditation of Laboratory Animal Care.

Methods

Cytotoxicity assay

In vitro cytotoxicity was assessed in tumor cells by a tetrazolium-based colorimetric assay, which takes advantage of the metabolic conversion of MTS (3-[4,5-dimethylthiazol-2-yl]-5-[3-carboxymethoxyphenyl]-2-[4-sulphenyl]-2H-tetrazolium, inner salt) to a reduced form that absorbs light at 492 nm [30]. Cells were seeded 24 h prior to drug addition. Following a 72-h incubation at 37°C with serially diluted compound, MTS was added to the cells, in combination with the electron-coupling agent phenazine methosulfate. The incubation was continued for 3 h, after which the absorbency of the medium at 492 nm was measured with a spectrophotometer to obtain the number of surviving cells relative to control populations. The in vitro cytotoxicity of ixabepilone was evaluated in three tissue-specific tumor cell line panels: breast (35 lines), colon (20 lines), and lung (23 lines); the results are expressed as IC_{50} values.

Clonogenic cell survival assay

The potency with which ixabepilone kills clonogenic tumor cells (cells that are able to divide indefinitely to form a colony) in proliferating and nonproliferating states in vitro was evaluated by a colony-formation assay. Following 16 h of drug exposure, cells were trypsinized, plated at various densities, and allowed to form colonies. After 10 days of colony formation, cell colonies were stained with crystal violet solution for 5 min, allowed to dry, and then counted. The concentration needed to kill 90% of clonogenic cancer cells (IC_{90}) was determined.

Cellular uptake of paclitaxel and ixabepilone in HCT116 and HCT116/VM46 cell lines

Cells were seeded at a density of 3×10^5 cells in a T75 flask with RPMI 1640 medium containing 10% FBS and 25 mM HEPES buffer. Cells were grown in a 37°C CO_2 incubator with 5% CO_2 for 2 days. On Day 2, supernatants were removed from the flask and 10 mL of complete medium containing 20 nM paclitaxel or 20 nM ixabepilone was added to the flasks. At 10, 30 min; 1, 2, and 17 h after drug treatment, drugs were removed from the flask and the cells were washed with cold PBS. Cells were removed from the flask by trypsinization at room temperature. The cell pellets were quickly frozen on dry ice until determination of cellular uptake by high pressure liquid chromatography/mass spectrometry (HPLC/MS) analysis.

Determination of cellular drug uptake by HPLC/MS

Cell pellet samples (20 μL) were mechanically disrupted and then deproteinized with two volumes of acetonitrile containing 2 μg/mL BMS-188797 as internal standard (IS). After centrifugation to remove precipitated protein, a 10 μL portion of clear supernatant was analyzed by HPLC/MS/MS (Hewlett Packard model 1100 HPLC/Autosampler combination). The column used was a Phenomenex Luna Phenyl-Hexyl, 2 mm × 50 mm, 3 μm particles, maintained at 40°C and a flow rate of 0.5 mL/min. The mobile phase consisted of 5 mM ammonium formate in 90% water/10% acetonitrile (at pH 3.75) (A) and acetonitrile (B). The initial mobile phase composition was 75% A, 25% B, ramped to 35% B in 1 min, followed by a second ramp to 40% B over 3 min. A final increase to 60% B was performed over 1 min and held until all components were eluted. The HPLC was interfaced to a Finnigan LCQ Advantage ion-trap mass spectrometer operated in the positive ion electrospray, full MS/MS mode. For ixabepilone, fragmentation of m/z 507 yielded daughter ions for quantitation at m/z 420. For paclitaxel, fragmentation of m/z 876 (sodium adduct of taxol) yielded daughter ions for quantitation at m/z 591.1. For the IS, m/z 870 was fragmented to yield daughters at m/z 525. Helium was the collision gas. The retention times for ixabepilone, paclitaxel, and the IS were 2.49, 5.46, and 5.83 min, respectively. The standard curve ranged from 4 nM to 6.3 μM and was fitted with a quadratic regression weighted by reciprocal concentration (1/x). Limit of quantitation (LOQ) for the purposes of this assay was 10 nM. Quality

control samples at two levels in the range of the standard curve were used to accept individual analytical sets.

In vivo antitumor testing

The human tumors were maintained in BALB/c nu/nu nude or Beige-SCID mice. In C3H mice, 16/C and 16C/ADR tumors were maintained. Tumors were propagated as SC transplants in the appropriate mouse strain using tumor fragments obtained from donor mice. Tumor passage occurred biweekly for murine tumors and approximately every 2–8 weeks for the various human tumor lines.

Each of the required number of animals needed to detect a meaningful response was given an SC implant of a tumor fragment (~ 50 mg) with a 13-gauge trocar. For treatment of early-stage tumors, the animals were pooled before distribution to the various treatment and control groups. For treatment of animals with advanced-stage disease, tumors were allowed to grow to the predetermined size window, and animals were evenly distributed to various treatment and control groups. Tumors outside the predetermined size range were excluded from analysis. Treatment of each animal was based on individual body weight. Treated animals were checked daily for treatment-related toxicity/mortality. Each group of animals was weighed before the initiation of treatment (weight 1) and then again following the last treatment dose (weight 2). The difference in body weight (weight 2 − weight 1) provided a measure of treatment-related toxicity.

Tumor response was determined by measurement of tumors with a caliper twice a week, until the tumors reached a predetermined "target" size of 500 or 1,000 mg. Tumor weight, in mg, was estimated from the formula:

$$\text{Tumor weight} = (\text{length} \times \text{width}^2)/2.$$

Antitumor activity was evaluated at the maximum tolerated dose (MTD), defined as the dose level immediately below which excessive toxicity (i.e., more than one death) occurred. The MTD was frequently equivalent to overdose. When death occurred, the day of death was recorded. Treated mice that died prior to having their tumors reach target size were considered to have died from drug toxicity. Treatment groups with more than one death caused by drug toxicity were considered to have had excessively toxic treatments, and their data were not included in the evaluation of a compound's antitumor activity.

Tumor response endpoint was expressed in terms of tumor growth delay ($T - C$ value), defined as the difference in time in days required for the treated tumors (T) to reach a predetermined target size compared with those of the control group (C).

To estimate tumor cell kill (TCK) [log cell kill (LCK)], the tumor volume doubling time (TVDT) was first calculated with the formula:

$$\text{TVDT} = [\text{median time in days for control tumors to reach target size}]$$
$$- [\text{median time in days for control tumors to reach half the target size}].$$

The LCK was then determined as follows:

$$\text{LCK} = T - C/(3.32 \times \text{TVDT})$$

where indicated, tumor response was also characterized as partial regression (PR), complete regression (CR), or "long-term absence of measurable disease"; PR was defined as a decrease in tumor volume by $> 50\%$ from pretreatment volume, and CR was defined as the disappearance of any visible or palpable tumor mass for 2 consecutive tumor measurements. "Long-term absence of measurable disease" was defined as the disappearance of any visible or palpable tumor mass for a period greater than ten times the TVDT. Statistical evaluations of the data were performed using Gehan's generalized Wilcoxon test [31].

Head-to-head comparison of ixabepilone and paclitaxel against MDR breast cancer models

Head-to-head comparative studies were conducted to determine the relative antitumor efficacies of ixabepilone and paclitaxel against two P-gp-positive MDR breast cancer models: Note that 16C/ADR and MCF7/ADR, 16C/ADR, and MCF7/ADR breast cancer xenografts were derived as previously described [32]. Briefly, tumor 16C xenograft-bearing animals were dosed with adriamycin (ADR) (12 mg/kg) until tumors developed repression, but not long-term absence, of measurable disease. Treatments were continued for repeated cycles until no further repression was seen and 16C tumors were ADR resistant. The MCF-7/ADR model was provided by the National Cancer Institute (NCI). Head-to-head potency comparisons of ixabepilone and docetaxel were also performed using the same methodology as above, but using the paclitaxel-resistant, Pat-21 breast xenograft model.

Pharmacokinetic analysis

The pharmacokinetic analysis was conducted on female BALB/c nu/nu nude mice, aged 6–8 weeks. For drug administration, ixabepilone was first dissolved in a mixture of Cremophor®/ethanol (50:50), and then diluted 1:4 with 5% dextrose to the required dosage strength less than 1 h before drug administration. Mice were injected

intravenously (IV) through the tail vein at a volume of 0.01 mL/gm.

Each timepoint contained three mice, and blood samples were collected by cardiac puncture. Plasma was obtained by centrifugation, and the supernatant and standards were deproteinized by the addition of two volumes of acetonitrile containing the IS, epothilone A. The supernatant was analyzed by HPLC/MS/MS, using a Phenomenex Prodigy C18-ODS3 column, 2 mm × 100 mm, 3 μm particles, maintained at 40°C and a flow rate of 0.3 mL/min. The mobile phase consisted of 5 mM ammonium acetate in 90% water/10% acetonitrile (A) and 5 mM ammonium acetate in 10% water/90% acetonitrile (B). The initial mobile phase composition was 70% A/30% B over 5 min, and was held at that composition for an additional 6 min. The mobile phase was then returned to initial conditions and the column re-equilibrated. The HPLC was interfaced to a Finnigan LCQ ion-trap mass spectrometer operated in the positive electrospray, full MS/MS mode. For ixabepilone, fragmentation of m/z 507 yielded daughter ions for quantitation at m/z values of 320, 402, and 420. For the IS, m/z 594 was fragmented to yield daughters for quantitation at m/z values of 406, 506, and 576. Helium was the collision gas. The retention times for ixabepilone and the IS were 8.3 and 10.4, respectively. The standard curve ranged from 10 nM to 40 μM and was fitted with a quadratic regression weighted by reciprocal concentration (1/x). The level of quantification and quality control were as previously described for cellular uptake experiments.

The area under the plasma ixabepilone concentration-time curve (AUC) was calculated using the trapezoidal method and extrapolated to infinity. The terminal slope for the plasma concentration-time curve was derived by linear regression after log transformation of the plasma concentrations, and this slope was used in the extrapolation of the AUC to infinity and estimation of the terminal half-life. The total body clearance was derived from the dose/$AUC_{0-infinity}$, and the volume of distribution at steady state (Vd_{ss}) was calculated from the area under the moment curve extrapolated to infinity.

Results

Ixabepilone demonstrates broad antitumor activity in vitro and in vivo

In vitro cytotoxic activity of ixabepilone

In vitro assays in a panel of almost 80 breast, colon, and lung tumor cell lines demonstrated potent cytotoxic activity for ixabepilone. Figure 1a summarizes the results from 35 human breast cancer cell lines in which ixabepilone demonstrated potent cytotoxicity, with the majority of the IC_{50} values between 1.4 and 45.7 nM. Only four of 35 cell lines exhibited significant resistance, as evidenced by IC_{50} values in the range > 100 nM. A series of 20 human colon tumor cell lines were also shown to be highly sensitive to ixabepilone, with most IC_{50} values ranging from 4.7 to 49.7 nM; only two cell lines had IC_{50} values that approached or exceeded 100 nM (Fig. 1b). Finally, in a panel of 23 human lung carcinoma cell lines (Fig. 1c), all were shown to be sensitive to ixabepilone, with IC_{50} values in the range of 2.3–19.2 nM.

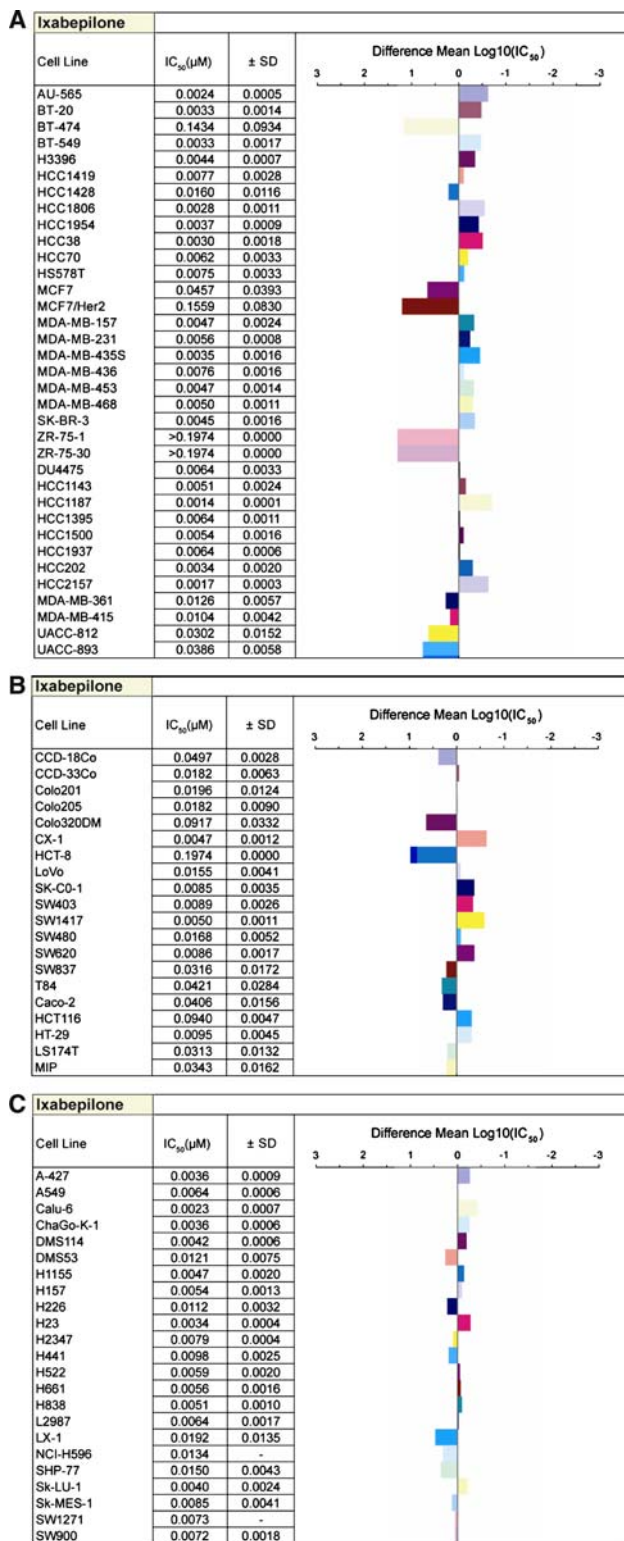#### In vivo antitumor testing

In vivo evaluation of ixabepilone mirrored the in vitro data described above, with robust antitumor activity demonstrated against a wide array of human cancer xenografts in nude mice. Ixabepilone demonstrated significant antitumor activity in 33 of 35 human cancer xenografts evaluated [consisting of eight breast, four non-small cell lung cancer (NSCLC), four pancreatic, eight ovarian, four prostate, four colon, one small cell lung cancer (SCLC), one gastric, and one squamous cell carcinoma xenograft] (Table 1). In the majority of tumors, prolonged tumor growth delay ≥ 1 LCK was achieved. This was accompanied by significant tumor regression rates, both partial and complete. In addition, in about 50% of tumor types, "long-term absence of measurable disease" was observed (Table 1). No treated mice died bearing tumors less than target size, indicating acceptable toxicity of the treatment administered.

Ixabepilone demonstrates greater activity in chemotherapy-resistant models compared with taxanes

Ixabepilone is more active than paclitaxel in P-gp-resistant breast cancer models

Having demonstrated the robust antitumor activity of ixabepilone against the range of in vivo human xenografts described above, it was important to establish whether activity was maintained in models displaying MDR. Consequently, head-to-head comparative studies were conducted in mice to determine the relative antitumor efficacy of ixabepilone and paclitaxel against two P-gp-positive MDR breast cancer models, 16C/ADR and MCF7/ADR (Table 2). Ixabepilone was significantly more active than paclitaxel in the 16C/ADR model ($P = 0.0048$). In the MCF7/ADR model, ixabepilone produced 0.5 LCK, compared with 0 LCK for paclitaxel; the difference between the two treatments was statistically significant ($P = 0.04$). These data are in agreement with previous

A Ixabepilone

Cell Line	IC$_{50}$(μM)	± SD
AU-565	0.0024	0.0005
BT-20	0.0033	0.0014
BT-474	0.1434	0.0934
BT-549	0.0033	0.0017
H3396	0.0044	0.0007
HCC1419	0.0077	0.0028
HCC1428	0.0160	0.0116
HCC1806	0.0028	0.0011
HCC1954	0.0037	0.0009
HCC38	0.0030	0.0018
HCC70	0.0062	0.0033
HS578T	0.0075	0.0033
MCF7	0.0457	0.0393
MCF7/Her2	0.1559	0.0830
MDA-MB-157	0.0047	0.0024
MDA-MB-231	0.0056	0.0008
MDA-MB-435S	0.0035	0.0016
MDA-MB-436	0.0076	0.0016
MDA-MB-453	0.0047	0.0014
MDA-MB-468	0.0050	0.0011
SK-BR-3	0.0045	0.0016
ZR-75-1	>0.1974	0.0000
ZR-75-30	>0.1974	0.0000
DU4475	0.0064	0.0033
HCC1143	0.0051	0.0024
HCC1187	0.0014	0.0001
HCC1395	0.0064	0.0011
HCC1500	0.0054	0.0016
HCC1937	0.0064	0.0006
HCC202	0.0034	0.0020
HCC2157	0.0017	0.0003
MDA-MB-361	0.0126	0.0057
MDA-MB-415	0.0104	0.0042
UACC-812	0.0302	0.0152
UACC-893	0.0386	0.0058

B Ixabepilone

Cell Line	IC$_{50}$(μM)	± SD
CCD-18Co	0.0497	0.0028
CCD-33Co	0.0182	0.0063
Colo201	0.0196	0.0124
Colo205	0.0182	0.0090
Colo320DM	0.0917	0.0332
CX-1	0.0047	0.0012
HCT-8	0.1974	0.0000
LoVo	0.0155	0.0041
SK-C0-1	0.0085	0.0035
SW403	0.0089	0.0026
SW1417	0.0050	0.0011
SW480	0.0168	0.0052
SW620	0.0086	0.0017
SW837	0.0316	0.0172
T84	0.0421	0.0284
Caco-2	0.0406	0.0156
HCT116	0.0940	0.0047
HT-29	0.0095	0.0045
LS174T	0.0313	0.0132
MIP	0.0343	0.0162

C Ixabepilone

Cell Line	IC$_{50}$(μM)	± SD
A-427	0.0036	0.0009
A549	0.0064	0.0006
Calu-6	0.0023	0.0007
ChaGo-K-1	0.0036	0.0006
DMS114	0.0042	0.0006
DMS53	0.0121	0.0075
H1155	0.0047	0.0020
H157	0.0054	0.0013
H226	0.0112	0.0032
H23	0.0034	0.0004
H2347	0.0079	0.0004
H441	0.0098	0.0025
H522	0.0059	0.0020
H661	0.0056	0.0016
H838	0.0051	0.0010
L2987	0.0064	0.0017
LX-1	0.0192	0.0135
NCI-H596	0.0134	-
SHP-77	0.0150	0.0043
Sk-LU-1	0.0040	0.0024
Sk-MES-1	0.0085	0.0041
SW1271	0.0073	-
SW900	0.0072	0.0018

◄ **Fig. 1 a** Cytotoxicity spectrum of ixabepilone against a panel of human breast cancer cell lines. Individual IC$_{50}$ results are the mean ± standard deviation (*SD*) from ≥3 separate experiments. Breast cell panel evaluation was performed in two separate stages: stage 1 = cell lines 1–23 (mean panel IC$_{50}$ value 0.0098 μM); and stage 2 = cell lines 24–35 (mean panel IC$_{50}$ value 0.0067 μM). The mean bar graph depicts the difference between the log of the individual cell line IC$_{50}$ values relative to the mean log of all of the IC$_{50}$ values. *Left-projecting bars* show resistant cell lines. **b** Cytotoxicity spectrum of ixabepilone against a panel of human colon cancer cell lines. Individual IC$_{50}$ results are the mean ± SD from ≥3 separate experiments. The mean colon panel IC$_{50}$ value was 0.0201 μM. The mean bar graph depicts the difference between the log of the individual cell line IC$_{50}$ values relative to the mean log of all of the IC$_{50}$ values. *Left-projecting bars* show resistant cell lines. **c** Cytotoxicity spectrum of ixabepilone against a panel of human lung cancer cell lines. Individual IC$_{50}$ results are the mean ± SD from ≥3 separate experiments. The mean lung panel IC$_{50}$ value was 0.0065 μM. The mean bar graph depicts the difference between the log of the individual cell line IC$_{50}$ values relative to the mean log of all of the IC$_{50}$ values. *Left-projecting bars* show resistant cell lines

Ixabepilone is more active than paclitaxel in P-gp-resistant colon cancer models

The parent HCT116 human colon carcinoma cell line and its P-gp overexpressing variant HCT116/VM46 were tested for sensitivity to paclitaxel and ixabepilone using a colony formation assay (Fig. 2a). Based on IC$_{90}$ values, the P-gp (MDR1)-overexpressing HCT116/VM46 was 25-fold more resistant to paclitaxel compared with its parent line HCT116. In contrast, HCT116/VM46 was only 2.2-fold more resistant to ixabepilone compared with the parental HCT116 cells.

In order to determine whether this difference in relative cytotoxicity was due, at least in part, to differences in P-gp-mediated cellular uptake, intracellular drug concentrations were evaluated in both cell lines. Paclitaxel and ixabepilone were incubated with the parent HCT116 cells and the MDR variant HCT116/VM46 cells at the therapeutic concentration of 20 nM. Intracellular drug concentrations were assayed at interval from 0 to 17 h after drug incubation. The results of this evaluation demonstrated that, whereas both ixabepilone and paclitaxel accumulated significantly in HCT116 cells, ixabepilone accumulated far more effectively in HCT116/VM46 cells compared with paclitaxel (Fig. 2b, c, only data up to 2 h were shown, results at 17 h were similar to 2 h). Thus, the ratios of drug concentrations in HCT116 versus HCT116/VM46 cells at the end of the 2-h incubation period were 48 and 4, respectively, for paclitaxel and ixabepilone (Fig. 2d), reflecting the decreased susceptibility of the latter compound to the efflux mechanism mediated by P-gp. These results may contribute to the increased therapeutic effect of ixabepilone compared with paclitaxel in this MDR cell line. Interestingly, while ixabepilone and paclitaxel had comparable

findings that ixabepilone possessed significant antitumor activity against other paclitaxel-resistant carcinomas, where resistance is attributed either to P-gp overexpression (Pat-7) or a tubulin mutation (A2780Tax) [5].

Table 1 Antitumor efficacy of ixabepilone as monotherapy against human tumor subcutaneous xenografts in nude mice

Tumor name	Dose (mg/m^2)[a]	Schedule	Growth delay (days)	LCK	PR (%)	CR (%)	Long-term absence of measurable disease (%)
Breast							
BT-474	6	Q7d ×3	>128	>3.4	75	13	0
KPL-4	6	Q4d ×5	>66.5	>4.5	100	100	100
MCF7	10	Q4d ×3	54	2.7	57	0	0
MCF7/ADR	9	Q4d ×3	23.3	0.6	0	0	0
MDA-MB-231	13	Q4d ×3	40	3.0	50	38	13
MDA-MB-435	13	Q4d ×3	57.5	2.9	100	13	0
Pat-14	9	Q4d ×3	>76.5	>1.6	100	100	0
Pat-21	11.6	Q4d ×3	71	2.3	100	29	5
Lung							
A549	11	Q4d ×3	47.5	1.3	17	4	0
Calu-6	13	Q4d ×3	30.7	3.1	25	0	0
L2987	10	Q4d ×3	66.2	4	100	100	75
LX-1	10	Q4d ×3	>67	>7.5	100	38	0
Pancreas							
Pat-24	10	Q4d ×3	>45.8	>1.8	71	71	29
Pat-25	15	Q4d ×3	106	1.8	38	25	13
Pat-26	10	Q4d ×3	23.5	1.2	20	0	0
Pat-27	10	Q4d ×3	>76	>2.5	100	71	14
Ovarian							
A2780 s	16	Q4d ×3	>47.5	>5.3	100	50	50
A2780Tax	6.3	Q2d ×5	23	2.5	0	0	0
CD228	10	Q4d ×3	>165.8	>6.7	100	100	50
MW387	10	Q4d ×3	37.5	0.8	75	13	13
PA354	10	Q4d ×3	41.3	1.3	86	29	14
Pat-7	10	Q4d ×3	25	2.4	88	0	0
Pat-18	10	Q4d ×3	>90.3	>2.6	100	75	25
Pat-22	10	Q4d ×3	>156	>3.6	100	71	57
Prostate							
CWR-22	8	Q4d ×3	38.8	5.3	13	0	0
LuCap35	8	Q4d ×3	>28	>1	ND	ND	ND
MDA-PCa-2b	12	Q4d ×3	58	2.2	ND	ND	ND
PC3	12	Q4d ×3	69.5	4	100	50	13
Colon							
GEO	10	Q4d ×3	15	1.1	0	0	0
HCT-116	10	Q4d ×3	>47.5	>6.3	100	63	63
HCT-116/VM46	16	Q4d ×3	26.8	2	0	0	0
HT29	13	Q4d ×3	58.3	2.3	100	86	0
SCLC							
NCI-H69	13	Q4d ×3	>84.8	>7.3	100	88	75
Gastric							
N87	10	Q4d ×3	>101.5	>3.3	100	63	63
Squamous							
A431	13	Q4d ×3	20.5	1.5	38	13	13

CR complete response, *IV* intravenous, *LCK* log$_{10}$ cell kill, *MTD* maximum tolerated dose, *ND* not determined, *PR* partial response, *Q7/4d* every 7/4 days

[a] All treatments were IV and at the MTD

Table 2 Comparison of the antitumor efficacy of ixabepilone and paclitaxel against two P-gp-positive multidrug resistant breast carcinomas: 16C/ADR and MCF7/ADR

Tumor type	Treatment		Efficacy		P
	Drug	Dose[a] (mg/kg)	Growth delay[d]		
			LCK	Days	
16C/ADR	Ixabepilone	10[b]	3.5	23.5	0.0048
	Paclitaxel	36[c]	1.4	9	
MCF7/ADR	Ixabepilone	6.3[c]	0.5	16.5	0.04
	Paclitaxel	36[c]	0	0.8	

LCK $\log_{10}$ cell kill

[a] Maximum tolerated dose

[b] Regimen = IV, Q4D ×3

[c] Regimen = IV, Q2D ×5

[d] Target tumor size = 500 mg for MCF7/ADR and 1,000 mg for 16C/ADR

IC_{50} values against the non-MDR line HCT116 (Fig. 2a), the concentration of paclitaxel in these cells was approximately threefold higher than that of ixabepilone. This suggests that ixabepilone is more potent than paclitaxel, consistent with previous in vitro tubulin polymerization results [5].

Ixabepilone is more potent than docetaxel in Pat-21 xenografts

To evaluate further the activity of ixabepilone in resistant tumor models, a head-to-head study comparing the relative antitumor efficacy of ixabepilone and a second taxane, docetaxel, against a paclitaxel-resistant model was performed in mice. The model, Pat-21, was established from a breast tumor biopsy from a patient who failed paclitaxel therapy. The paclitaxel resistance of this model is attributable to overexpression of βIII-tubulin and a lack of βII-tubulin [6]. As shown in Fig. 3, the potency of ixabepilone in Pat-21 xenografts was at least threefold that of docetaxel; this between-treatment difference was statistically significant ($P < 0.003$). Furthermore, ixabepilone produced antitumor activity of 1.6 LCK; this was superior to docetaxel, which was inactive ($P = 0.003$).

Plasma pharmacokinetics of ixabepilone in mice

An understanding of plasma pharmacokinetics is important for designing dosages and schedules for chemotherapy regimens, to ensure that therapeutic doses are attainable, and to interpret responses to treatment. Therefore, the plasma concentration-time profile of ixabepilone was characterized in mice following administration of various

doses (4, 6, and 10 mg/kg). The pharmacokinetic profile was characterized by a steep decline during the first hour after IV administration of ixabepilone, followed by a more prolonged terminal elimination phase with a mean half-life of 13 and 16 h at 6 and 10 mg/kg, respectively (Fig. 4). The AUC increased with dose: 1.4, 2.9, and 4.4 μM × h for the 4, 6, and 10 mg/kg ixabepilone doses, respectively. The mean Vd_{ss} values were 37, 32, and 21 L/kg, and the maximum concentration (C_{max}) was 2.4, 9.0, and 8.0 μM after administration of 4, 6, and 10 mg/kg, respectively. These data are consistent with extensive tissue binding. Total body clearance of ixabepilone was rapid (5.1, 5.0, and 4.3 L/h/kg after administration of 4, 6, and 10 mg/kg, respectively), but did not appear to be dose-dependent.

Discussion

Tumor resistance to chemotherapeutic agents is a significant limitation of this treatment modality in many patients. The taxanes, for example, are susceptible to several mechanisms of tumor resistance, including MDR protein-mediated efflux, overexpression of βIII-tubulin isoform, and tubulin mutations. Because resistance to taxanes and other drug classes ultimately limits their efficacy, development of agents able to overcome any of these resistance mechanisms would address a significant clinical need.
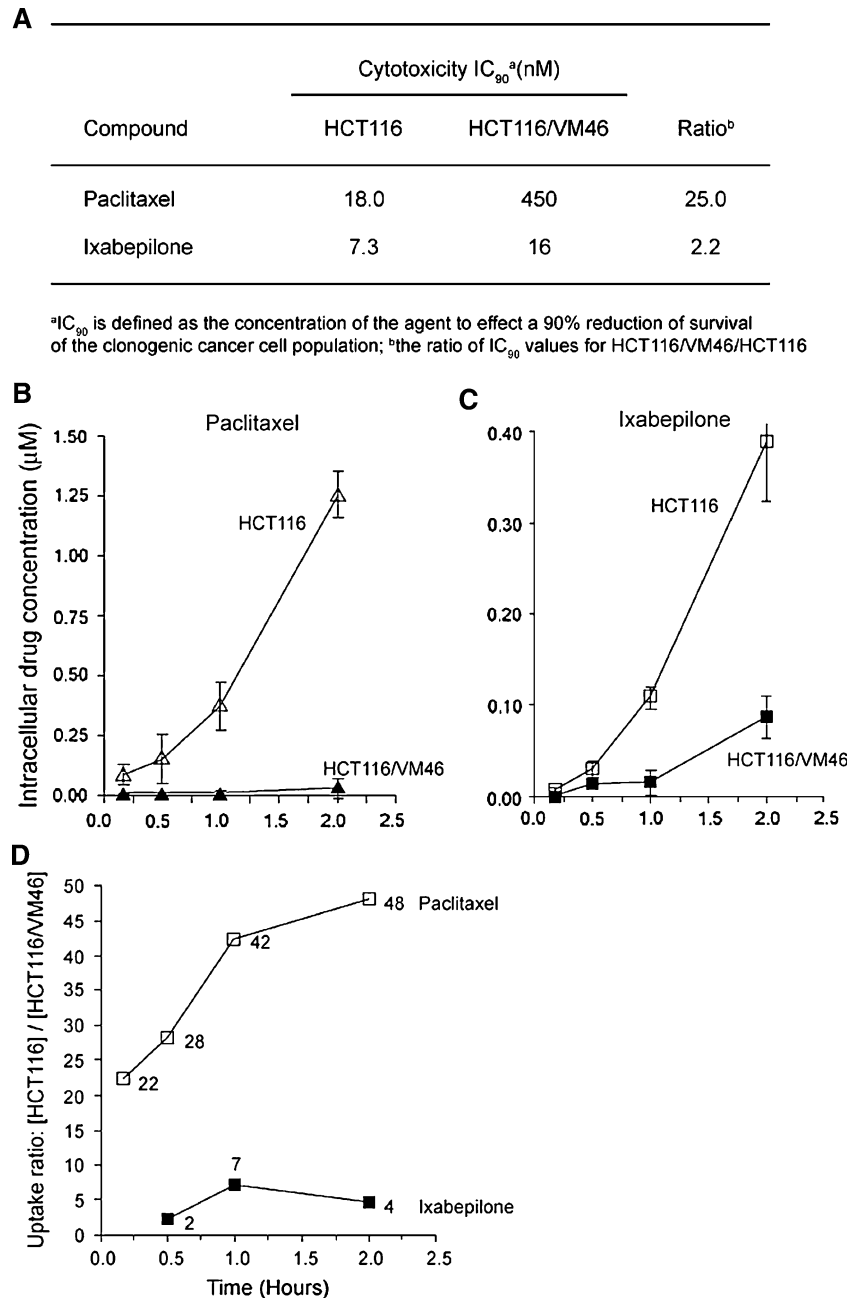
Results presented from these in vitro cytotoxicity studies against three different tissue-specific, cancer cell-line panels demonstrate that ixabepilone has potent and broad-spectrum antineoplastic activity. The effectiveness of ixabepilone in vitro is paralleled by equally broad-spectrum activity in vivo, with robust antitumor activity seen against 35 human tumor xenografts representing a wide array of tumor types including breast, colon, NSCLC, pancreatic, ovarian, prostate, SCLC, gastric, and squamous cell carcinomas. Furthermore, in 33 of 35 tumors, 1 LCK or greater efficacy was seen in addition to significant tumor regression rates, including "long-term absence of measurable disease" in ∼50% of the tumor types tested. Moreover, in agreement with previous studies [5, 6], ixabepilone demonstrated greater activity than taxanes in a range of models resistant to other chemotherapeutics due to various mechanisms, including overexpression of βIII-tubulin (e.g., Pat-21), overexpression of P-gp (e.g., Pat-7, HCT116/VM46), and tubulin mutations (e.g., A2780Tax ovarian carcinoma).

The activity of ixabepilone in these drug-resistant models can most likely be explained by the low susceptibility of ixabepilone to several mechanisms of drug resistance. For example, it was previously shown that ixabepilone displays reduced susceptibility to P-gp and other efflux pumps compared with the taxanes, and that

Fig. 2 Clonogenic cytotoxicity and differential cellular uptake of ixabepilone and paclitaxel in paclitaxel-resistant HCT116/VM46 P-gp-overexpressing colon carcinoma cell line. **a** Clonogenic cytotoxicity based on IC_{90} values in a clonogenic cell survival assay. **b** Paclitaxel and **c** ixabepilone uptake in HCT116 and HCT116/VM46 (P-gp overexpressing) human colon carcinoma cell lines. **d** Uptake ratios in HCT116 versus HCT116/VM46 for paclitaxel and ixabepilone


A

Compound	Cytotoxicity IC_{90}[a](nM)		Ratio[b]
	HCT116	HCT116/VM46	
Paclitaxel	18.0	450	25.0
Ixabepilone	7.3	16	2.2

[a]IC_{90} is defined as the concentration of the agent to effect a 90% reduction of survival of the clonogenic cancer cell population; [b]the ratio of IC_{90} values for HCT116/VM46/HCT116

ixabepilone does not induce expression of MDR proteins [5]. The cellular uptake of ixabepilone, but not paclitaxel, in P-gp-overexpressing cells shown in the present study supports this observation, and is consistent with the activity of ixabepilone in MDR models such as HCT116/VM46. Ixabepilone is also able to overcome resistance conferred by overexpression of the βIII-tubulin isoform, as exemplified by its activity in the paclitaxel-resistant Pat-21 model. The precise mechanism of Pat-21 resistance was unknown until quite recently. However, recent studies suggest that a combination of loss of βII-tubulin

and overexpression of βIII-tubulin may be responsible for the paclitaxel resistance of Pat-21 [6]. In the studies reported here, the head-to-head comparison of ixabepilone versus docetaxel in the Pat-21 model showed that ixabepilone was significantly more potent than docetaxel. The activity of ixabepilone against this taxane-resistant model may be explained by the fact that the tubulin-binding mode of ixabepilone affects the microtubule dynamics of multiple tubulin isoforms, including βIII-tubulin. Moreover, ixabepilone preferentially suppresses dynamic instability of $\alpha\beta$III-microtubules compared with
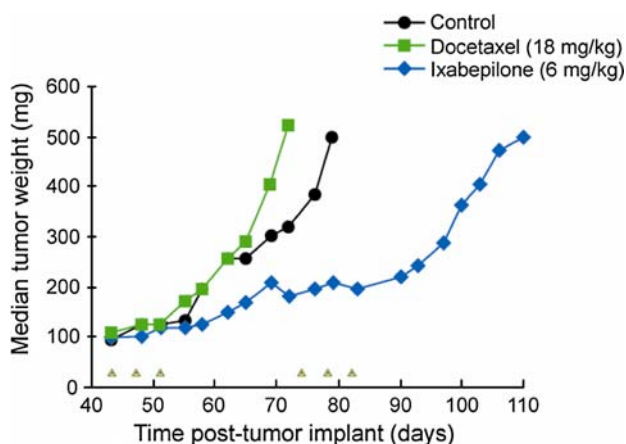
Fig. 3 Potency of ixabepilone compared with docetaxel in the paclitaxel-resistant Pat-21 xenograft model. Schedule was two courses of ixabepilone/docetaxel Q4d ×3 for two courses (Q4d: every 4 days)
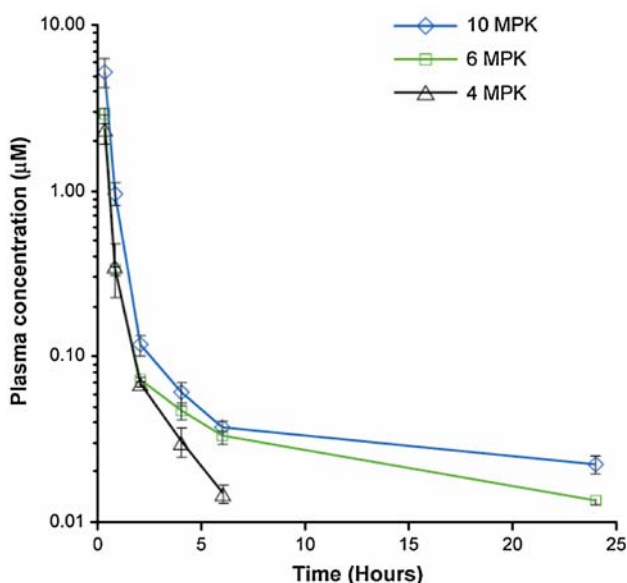
Fig. 4 Pharmacokinetics of ixabepilone. Mean plasma concentration (in log scale)—time profiles in nude mice treated with 4, 6, and 10 mg/kg ixabepilone

$\alpha\beta$II-microtubules [6]. Thus, the ability of ixabepilone to bind βIII-tubulin, and its preferential binding of βIII-tubulin over βII-tubulin, may explain the selective sensitivity of the Pat-21 model to ixabepilone.

An understanding of pharmacokinetic parameters for ixabepilone, along with its antitumor activity, allows for greater maintenance of overall effective drug concentration while minimizing toxicity. The pharmacokinetics of ixabepilone reported herein in mice are characterized by rapid tissue distribution and extensive tissue binding, as shown by the large Vd_{SS} (107 L/m^2) at a dose of 30 mg/m^2, which

corroborates the large Vd_{ss} (530–840 L/m^2) observed in humans administered the currently approved dosage of 40 mg/m^2 [33–35]. It was also important to establish the in vivo stability of ixabepilone to better understand the dynamics of its metabolism following administration. Importantly, the half-life of ixabepilone (13 h at 6 mg/kg and 16 h at 10 mg/kg) was considerably longer than that of desoxyepothilone B, which has a lactone at position 16 and a half-life in mice of approximately 20 min [36]. This suggests that replacing the lactone oxygen with a lactam improves the metabolic stability of the molecule through overcoming lactone hydrolysis by esterases in the mouse. Although there are reduced esterase levels in human compared with mouse plasma, P450-bearing microsomes in human liver are able to hydrolyze epothilone B lactone [37].

Therefore, it is likely that the lactam modification is important in extending the half-life of ixabepilone in humans. This is supported by the favorable half-life of ixabepilone in humans (35 h) seen in a phase I dose-finding study [33]. The favorable clinical pharmacokinetic characteristics of ixabepilone are further demonstrated by the finding in phase I clinical studies that AUC of ixabepilone at the approved dose of 40 mg/m^2 (1,760–2,560 ng h/ml, 3.5–5.1 μM h) was higher than that of patupilone (204–237 ng h/mL, over a range of administration schedules) [33–35, 38]. It is also worth noting that this exposure level is similar to those produced in mice at therapeutically efficacious doses (Fig. 4). Therefore, the overall pharmacokinetic profile of ixabepilone reported here and previously demonstrates that plasma levels of ixabepilone required for antitumor activity are attainable clinically.

Consistent with its favorable pharmacokinetics and notable preclinical activity in this study, promising clinical activity of ixabepilone has been seen against a wide range of tumor types, including breast [locally advanced (LABC) and metastatic (MBC)], lung, renal, prostate, pancreas, and lymphoma [16–28]. In several instances, tumors had been heavily pretreated or were resistant to current therapies, including anthracycline-pretreated MBC [25], taxane-resistant MBC [26], and MBC or LABC resistant to an anthracycline, a taxane, and capecitabine, [39] suggesting that the reduced susceptibility of ixabepilone to mechanisms of drug resistance seen in these and other preclinical studies can translate to the clinic.

In summary, ixabepilone has broad-spectrum in vitro and in vivo activity across a range of tumor types, accompanied by desirable pharmacokinetics. Consistent with its reduced susceptibility to several mechanisms of drug resistance, ixabepilone is active against a range of resistant tumor xenografts, including those resistant to taxanes. These preclinical findings have translated into clinical activity against a wide range of tumor types, including heavily pretreated and

drug-resistant tumors. One phase II neoadjuvant study has correlated response to ixabepilone in breast cancer patients with the expression of specific cellular genes such as *ER* [40]. In addition, a phase III study in patients with anthracycline- and taxane-resistant MBC demonstrated superior efficacy for ixabepilone in combination with capecitabine versus capecitabine alone, with 40% prolongation of PFS and 2.5-fold higher rate of response [41].

References

1. Longley D, Johnston P (2005) Molecular mechanisms of drug resistance. J Pathol 205:275–292

2. Moscow JMC, Cowan KH (2003) Drug resistance and its clinical circumvention. In: Kufe D, Pollock R, Weischselbaum R, Bast R, Gansler T, Holland J, Frei E (eds) Cancer medicine. BC Decker, Hamilton

3. Endicott JA, Ling V (1989) The biochemistry of P-glycoprotein-mediated multidrug resistance. Annu Rev Biochem 58:137–171

4. Gottesman MM, Pastan I (1993) Biochemistry of multidrug resistance mediated by the multidrug transporter. Annu Rev Biochem 62:385–427

5. Lee FYF, Borzilleri R, Fairchild CR, Kim S-H, Long BH, Raventoz-Suarez C, Vite GD, Rose WC, Kramer RA (2001) BMS-247550: a novel epothilone analog with a mode of action similar to paclitaxel but possessing superior antitumor activity. Clin Cancer Res 7:1429–1437

6. Jordan M, Miller H, Ni L, Castenada S, Inigo I, Kan D, Lewin A, Ryseck R, Kramer R, Wilson L, Lee FY (2006) The Pat-21 breast cancer model derived from a patient with primary Taxol® resistance recapitulates the phenotype of its origin, has altered beta-tubulin expression and is sensitive to ixabepilone. In: Proc Am assoc cancer res 97th annual meeting, LB-280

7. Altaha R, Fojo T, Reed E, Abraham J (2003) Epothilones: a novel class of non-taxane microtubule-stabilizing agents. Curr Pharm Des 8:1707–1712

8. Bollag DM, McQueney PA, Zhu J, Hensens O, Koupal L, Liesch J, Goetz M, Lazarides E, Woods CM (1995) Epothilones, a new class of microtubule-stabilizing agents with a Taxol-like mechanism of action. Cancer Res 55:2325–2333

9. Bode CJ, Gupta ML, Reiff EA, Suprenant KA, Georg GI, Himes RH (2002) Epothilone and paclitaxel: unexpected differences in promoting the assembly and stabilization of yeast microtubules. Biochemistry 41:3870–3874

10. Chou T-C, Zhang X-G, Bolag A, Su D-S, Meng D, Salvin K, Bertino J, Danishefsky SJ (1998) Desoxyepothilone B: an efficacious microtubule-targeted antitumor agent with a promising in vivo profile relative to epothilone B. Proc Natl Acad Sci USA 95:9642–9647

11. Lee F, Borzilerri R, fairchild C, Kamath A, Smykla R, Kramer R, Vite G (2008) Preclinical discovery of ixabepilone, a highly active antineoplastic agent. Cancer Chemother Pharmacol (in press)

12. Awada A, Burris D, de Valeriola D (2001) Phase I clinical and pharmacology study of the epothilone B analog BMS-247550 given weekly in patients with advanced solid tumors. Clin Cancer Res 7:3801S

13. Loruzzo P, Wozniak A, Flaherty L, Shields A, Wright J, Lebwhol D (2001) Phase I clinical trial of BMS-247550 (aka Epothilone B Analog; NSC710428) in adult patients with advanced solid tumors. Proc Am Soc Clin Oncol 20 (abstr. #2125)

14. Spriggs D, Soignet S, Bienvenu B, Letrent S, Lebwohl D, Jones S, Burris HI (2001) Phase I first-in-man study of the epothilone B analog BMS-247550 in patients with advanced cancer. Proc Am Soc Clin Oncol 20 (abstr. 428)

15. Hao D, Hammond LA, deBono JS, Tolcher AW, Berg KE, Bass A, Mays TA, Smith LS, Drengler R, Rowinsky EK (2002) Continuous weekly administration of the epothilone-B derivative, BMS247,550 (NSC710428): a phase I and pharmacokinetic (PK) study. Proc Am Soc Clin Oncol 21 (abstr. #411)

16. Ajani JA, Shah MA, Bokemeyer C, Lenz H-J, Burris HA, Cutsem EV, Usakewicz J, Peeters O, Voi M, Lebwohl D, Safran H (2002) Phase II study of the novel epothilone BMS-247550 in patients (pts) with metastatic gastric adenocarcinoma previously treated with a taxane. Proc Am Soc Clin Oncol 21 (abstr. 619)

17. Baselga J, Gianni L, Llombart A, Manikhas G, Kubista E, Steger G (2005) Predicting response to ixabepilone: genomics study in patients receiving single agent ixabepilone as neoadjuvant treatment for breast cancer (BC). Breast Cancer Res Treat 94:S31 (abstr. 305)

18. Fojo A, Menefee M, Poruchynsky M, Edgerly M, Mickley L, Li N, Tapia E, Merino M, Balis F, Bates S (2005) A translational study of ixabepilone (BMS-247550) in renal cell cancer (RCC): assessment of its activity and demonstration of target engagement in tumor cells. J Clin Oncol 23:388S (abstr 4541)

19. Galsky MD, Small EJ, Oh WK, Chen I, Smith DC, Colevas AD, Martone L, Curley T, DeLaCruz A, Scher HI, Kelly WK (2005) Multi-Institutional randomized phase II trial of the epothilone B analog ixabepilone (BMS-247550) with or without estramustine phosphate in patients with progressive castrate metastatic prostate cancer. J Clin Oncol 23:1439–1446

20. Hussain M, Tangen CM, Lara PN Jr, Vaishampayan UN, Petrylak DP, Colevas AD, Sakr WA, Crawford ED (2005) Ixabepilone (epothilone B analogue BMS-247550) is active in chemotherapy-naive patients with hormone-refractory prostate cancer: a Southwest Oncology Group Trial S0111. J Clin Oncol 23:8724–8729

21. O'Connor O, Straus D, Moskowitz C, Hamlin P, Portlock C, Gerecitano J, Neylon E, Colevas D, Zelenetz A (2005) Targeting the microtubule apparatus in indolent and mantle cell lymphoma with the novel epothilone analog BMS 247550 induces major and durable remissions in very drug resistant disease. J Clin Oncol 23:16S (abstr. 6569)

22. Smith SM, Pro B, Besien Kv, Conner K, Karrison T, Wong S, Stiff P, Vokes E (2005) A phase II study of epothilone B analog BMS-247550 (NSC 710428) in patients with relapsed aggressive non-Hodgkin's lymphomas. J Clin Oncol 23:16S (abstr. 6625)

23. Conte P, Thomas E, Martin M, Klimovsky J, Tabernero J (2006) Phase II study of ixabepilone in patients (pts) with taxane-resistant metastatic breast cancer (MBC): final report. J Clin Oncol 24:18S (abstr. 10505)

24. Whitehead RP, McCoy S, Rivkin SE, Gross HM, Conrad ME, Doolittle GC, Wolff RA, Goodwin JW, Dakhil SR, Abbruzzese JL (2006) A Phase II trial of epothilone B analogue BMS-247550 (NSC #710428) ixabepilone, in patients with advanced pancreas cancer: a Southwest Oncology Group study. Invest New Drugs 24:512–520

25. Roche H, Yelle L, Cognetti F, Mauriac L, Bunnell C, Sparano J, Kerbrat P, Delord J-P, Vahdat L, Peck R, Lebwohl D, Ezzeddine R, Cure H (2007) Phase II clinical trial of ixabepilone

(BMS-247550), an epothilone B analog, as first-line therapy in patients with metastatic breast cancer previously treated with anthracycline chemotherapy. J Clin Oncol 25:3415–3420

26. Thomas E, Tabernero J, Fornier M, Conte P, Fumoleau P, Lluch A, Vahdat LT, Bunnell CA, Burris HA, Viens P, Baselga J, Rivera E, Guarneri V, Poulart V, Klimovsky J, Lebwohl D, Martin M (2007) Phase II clinical trial of ixabepilone (BMS-247550), an epothilone B analog, in patients with taxane-resistant metastatic breast cancer. J Clin Oncol 25:3399–3406

27. Vansteenkiste J, Lara PN Jr, Le Chevalier T, Breton J-L, Bonomi P, Sandler AB, Socinski MA, Delbaldo C, McHenry B, Lebwohl D, Peck R, Edelman M (2007) Phase II clinical trial of the epothilone B analog, ixabepilone, in patients with non small-cell lung cancer whose tumors have failed first-line platinum-based chemotherapy. J Clin Oncol 25:3448–3455

28. Zhuang SH, Hung YE, Hung L, Robey RW, Sackett DL, Linehan WM, Bates SE, Fojo T, Poruchynsky MS (2007) Evidence for microtubule target engagement in tumors of patients receiving ixabepilone. Clin Cancer Res 13:7480–7486

29. Long BH, Wang L, Lorico A, Wang RRC, Brattain MG, Casazza AM (1991) Mechanisms of resistance to etoposide and teniposide in acquired resistant human colon and lung carcinoma cell lines. Cancer Res 51:5275–5284

30. Riss TL, Moravec RA (1992) Comparison of MTT, XTT, and a novel tetrazolium compound MTS for in vitro proliferation and chemosensitivity assays. Mol Biol Cell 3(Suppl):184a

31. Gehan EA (1965) A generalized Wilcoxon test for comparing arbitrarily singly-censored samples. Biometrika 52:203–223

32. Lee F, Sciandra J, Siemann D (1989) A study of the mechanism of resistance to Adriamycin in vivo. Glutathione metabolism, P-glycoprotein expression and drug transport. Biochem Pharmacol 38:3697–3705

33. Mani S, McDaid H, Hamilton A, Hochster H, Cohen MB, Khabelle D, Griffin T, Lebwohl DE, Liebes L, Muggia F, Horwitz SB (2004) Phase I clinical and pharmacokinetic study of BMS-247550, a novel derivative of epothilone B, in solid tumors. Clin Cancer Res 10:1289–1298

34. Gadgeel SM, Wozniak A, Boinpally RR, Wiegand R, Heilbrun LK, Jain V, Parchment R, Colevas D, Cohen MB, LoRusso PM (2005) Phase I clinical trial of BMS-247550, a derivative of epothilone B, using accelerated titration 2B design. Clin Cancer Res 11:6233–6239

35. Aghajanian C, Burris HA III, Jones S, Spriggs DR, Cohen MB, Peck R, Sabbatini P, Hensley ML, Greco FA, Dupont J, O'Connor OA (2007) Phase I study of the novel epothilone analog ixabepilone (BMS-247550) in patients with advanced solid tumors and lymphomas. J Clin Oncol 25:1082–1088

36. Chou T-C, O'Connor OA, Tong WP, Guan Y, Zhang Z-G, Stachel SJ, Lee C, Danishefsky SJ (2001) The synthesis, discovery, and development of a highly promising class of microtubule stabilization agents: curative effects of desoxyepothilones B and F against human tumor xenografts in nude mice. PNAS 98:8113–8118

37. Lee FYF, Vite GD, Hofle G, Kim SH, Clark J, Fager K, Kennedy K, Smykla R, Wen M, Leavitt K, Johnston KA, Peterson RW, Kamath A, Franchini M, Schulze G, Fairchild C, Raghavan K, Long BH, Kramer R (2002) The discovery of BMS-310705: a water-soluble and chemically stable semi-synthetic epothilone possessing potent parenteral and oral antitumor activity against models of taxane-sensitive and -resistant human tumors in vivo. Proc Am Assoic Cancer Res 43:792–793

38. Rubin EH, Rothermel J, Tesfaye F, Chen T, Hubert M, Ho Y-Y, Hsu C-H, Oza AM (2005) Phase I dose-finding study of weekly single-agent patupilone in patients with advanced solid tumors. J Clin Oncol 23:9120–9129

39. Perez EA, Lerzo G, Pivot X, Thomas E, Vahdat L, Bosserman L, Viens P, Cai C, Mullaney B, Peck R, Hortobagyi GN (2007) Efficacy and safety of ixabepilone (BMS-247550) in a phase II study of patients with advanced breast cancer resistant to an anthracycline, a taxane, and capecitabine. J Clin Oncol 25:3407–3414

40. Lee H, Xu L, Wu S, Paul B, Baselga J, Llombart A, Steger GG, Galbraith S, Clark E (2006) Predictive biomarker discovery and validation for the targeted chemotherapeutic ixabepilone. J Clin Oncol 24:18S (abstr. 3011)

41. Thomas ES, Gomez HL, Li RK, Chung H-C, Fein LE, Chan VF, Jassem J, Pivot XB, Klimovsky JV, de Mendoza FH, Xu B, Campone M, Lerzo GL, Peck RA, Mukhopadhyay P, Vahdat LT, Roche HH (2007) Ixabepilone plus capecitabine for metastatic breast cancer progressing after anthracycline and taxane treatment. J Clin Oncol 25:5210–5217